Validation of insulated joints

Master's Thesis in Solid and Fluid Mechanics

ANTON WAHNSTRÖM

Department of Applied Mechanics
Division of Material and Computational Mechanics
CHALMERS UNIVERSITY OF TECHNOLOGY
Gothenburg, Sweden 2011
Master's Thesis 2011:04

MASTER'S THESIS 2011:04

Validation of insulated joints

Master's Thesis in Solid and Fluid Mechanics

ANTON WAHNSTRÖM

Department of Applied Mechanics
Division of Material and Computational Mechanics
CHALMERS UNIVERSITY OF TECHNOLOGY

Gothenburg, Sweden 2011

Validation of insulated joints
ANTON WAHNSTRÖM

Master's Thesis 2011:04
ISSN 1652-8557
Department of Applied Mechanics
Division of Material and Computational Mechanics
Chalmers University of Technology
SE-412 96 Gothenburg
Sweden
Telephone: + 46 (0)31-772 1000

Chalmers Reproservice
Gothenburg, Sweden 2011

Validation of insulated joints
Master's Thesis in Solid and Fluid Mechanics
ANTON WAHNSTRÖM
Department of Applied Mechanics
Division of Material and Computational Mechanics

Chalmers University of Technology

Abstract

In track engineering, insulated joints are widely used as a key component in the signaling system to electrically insulate track sections and thereby locate trains. However, many problems with track deterioration and signaling malfunction are related to them. In spite of this, the requirements on validation testing to assure the mechanical quality of insulated joints are rather low. Trafikverket (Swedish Transport Administration) has a standard that specifies tension tests for insulated joints. However the related bending test is not specified, which makes comparisons between tests cumbersome. There is therefore a need to establish a standardized bending test to compare and evaluate the quality of insulated joints. This thesis outlines such a standardized test.

Further, a crucial part in the validation is operational testing. This thesis scrutinizes the issue of how tests should be designed to assure a high statistical confidence.

Keywords: Insulated joints, bending test

Contents

Abstract **I**

Contents **III**

Preface **V**

1 Introduction **1**
1.1 Background 1
1.2 Method 1
1.3 Function of an insulated joint 1
1.4 Common joint damages 1
1.5 Limitations 3

2 Approach **4**
2.1 Mesh influence 4
2.2 Investigated parameters 8

3 Load modeling **9**
3.1 Single and double axle bogies 9
3.2 Dynamic load effects 12
3.3 Rail profile 12
3.4 Joint position 12
3.5 Insulation material 13
3.6 Test specimen 13
3.7 Error margins 14

4 Test setup **16**
4.1 Test procedure 16

5 Evaluation of field validation tests **21**
5.1 Determining which joint type that has the highest quality 21
5.2 Quality factor comparison 23
5.3 Mean life estimation 25
5.3.1 Mean life time estimation, five joints of each type 26
5.3.2 Mean life time estimation, 15 joints of each type 26
5.4 Some simplifications and assumptions made in the above study 26

6 Concluding remarks **28**
6.1 Laboratory test set-up 28
6.2 Validation tests 28

7 Appendix **29**

Here you can add preface and notations

Preface

This thesis work was carried out 2010-2011 at Chalmers University of Technology, Department of Applied Mechanics. It was made following an inquiry from Swedish Traffic Administration (Trafikverket).

I would like to thank Anders Ekberg, Fredrik Jansson, Elena Kabo and Johan Sandström for invaluable help during the project.

Gothenburg March 2011
Anton Wahnström

1 Introduction

To obtain a sustainable development the transport system in general rail traffic in particular is of significant interest. There is therefor a need for increasing the quality of the rail operation to achieve higher reliability and capacity. One important component in the rail system is the insulated joint. The purpose of this project is to develop methods to increase the quality of the joint designs.

1.1 Background

Requirements on insulated joints are, in spite of their importance and frequent use, rather low. In Sweden there is a standard for specification of tension tests for insulated joints [7], but yet no standard for bending test. To increase the quality of the insulating joints there is therefore a need to develop a standard for bending tests.

In addition to the bending test, methods for field validation of joints has been developed. The algorithms that are used are not specific for insulating joints and can therefore be applied to other kinds of statistical evaluation of tests.

1.2 Method

A finite element model of the track has been developed [5] and calibrated towards the characteristics of the track. The model was initially designed to evaluate the dynamic characteristics of the track but has in this project instead been used to compute the track's quasi-static responses. In the finite element program Abaqus the model was adopted for a variety of situations and from this it was possible to determine the influence of different parameters such as single or double bogie, boundary conditions, length of test specimen etc.

1.3 Function of an insulated joint

The common signaling layout of a track consists of one un-sectioned rail (grounding rail), while the other rail is sectioned (with each section in normal cases around 1–2 kilometers long) by insulated joints (see figure 1.1). A low voltage is applied to the rail section between the joints. A wheelset will short-circuit the rails, whereby the vehicle can be detected and the signaling system and thereby prevent other trains from entering the area. If the insulated joint is short-circuited e.g. by detached metal chips the two adjacent rail sections will from a signaling point of view act as one. Thus, it cannot be determined on which of these two sections the vehicle is located. This causes operational disturbances. Nota bene, a short-circuited joint can signal that a train is located on a section where it's not, but it will not indicate a free section if there is a train on it.

1.4 Common joint damages

Several problems can affect insulated joints, including:

- cracked fishplates, usually initiated at the bolt holes (figures 1.2 and 1.3)
- plastic deformation, wear and fatigue damage in the vicinity of the insulated joint These damages can cause detachment of metal flakes and subsequent short-circuiting
- detachment of the insulating layer from the rail ends

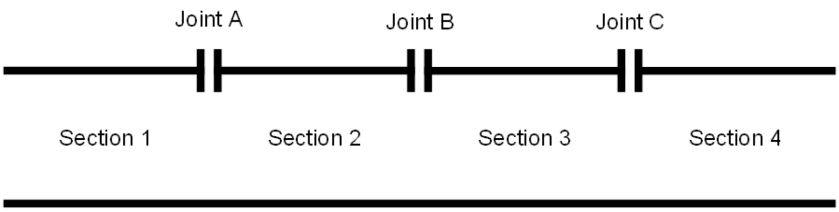

Figure 1.1: Insulated joints and sections.

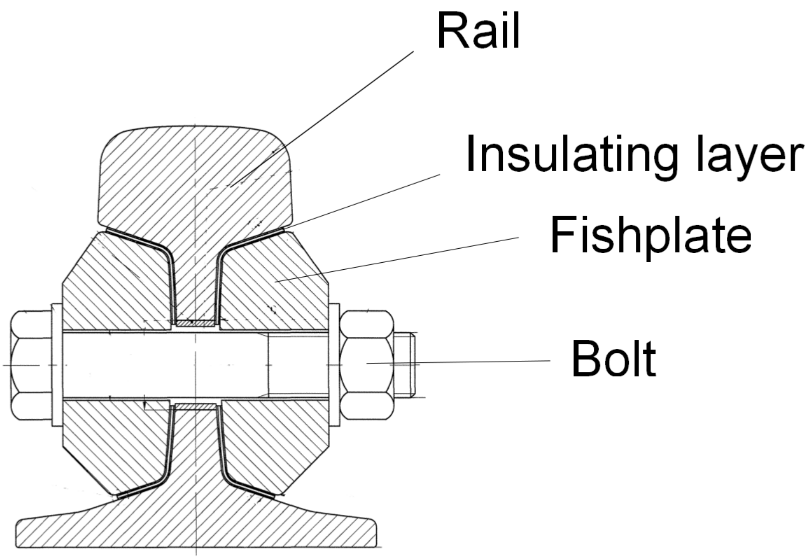

Figure 1.2: Cross-section view of an insulated joint.

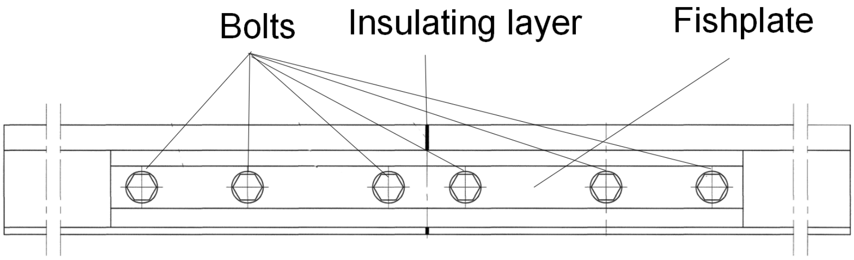

Figure 1.3: Side view of an insulated joint.

- macro-scale dipping of the insulating joint due to settling of the supporting sleepers, and also plastic deformation, wear etc. of the rail edge at the insulating layer

To evaluate the costs of an insulated joint one has to take into account the probability and related costs of all possible problems related to the joint.

The root cause of the problems listed above is the mechanical loading of passing trains as well as stresses and strains due to restrained temperature expansion. The mechanical loading can be considered both as a contact stress field (of relevance close to the point of contact), rail bending due to passing wheels, and longitudinal rail forces due to restricted thermal contraction/expansion and traction/breaking of the wheels. In this project only mechanical deterioration related to bending is investigated. Nevertheless it is important to bear in mind also the other related phenomena since it is not economically feasible to sub-optimize a joint solely with respect to bending properties.

1.5 Limitations

On of the project's aim is to develop a method for comparing the bending strength of insulated joints by laboratory experiments. The method is restricted to evaluate bending strength and therefore other tests will be needed to determine longitude tensile strength and/or electrical insulation properties. The aim is not to deduce what material in rail and joint that should be used. No economical analysis is carried out in the project, however the results can serve as background for refined such analyses since it facilitates predictions of lifetimes of insulated joints.

The model does not account for factors such as dynamic effects, the direction of passing vehicles or the acceleration or braking of passing trains. If the joint is located close to a station the train will accelerate or brake in while passing the joint, causing unsymmetrical wear on the joint region. The altered shape of the joint can increase the dynamical effects and thereby shift the locations where forces and moments are the highest. This is however not covered in this project but it might be considered as a follow-up project. Finally the proposed solutions are scrutinized in the light of a proposed CEN norm. In particular, differences are highlighted and motivations for the suggestions in the current report are given.

In addition the project aims at outlining guidelines for validation of insulated joints by field tests.

2 Approach

The numerical model was developed in the finite element code Abaqus [9]. A structural model as detailed in [5] was employed. The geometry of the structure is shown in figure 2.1, *rail 1* is the rail where the joint is located, and *rail 2* is the continuous rail. To facilitate computations, it was assumed that the beams in the structure responded purely elastically.

The railtype used in the calculations is, if nothing else is stated, BV50.

The ballast is modeled as an elastic foundation in Abaqus, with $k_z = 2.4 \cdot 10^7 \text{N/m}^2$. The railpads are modeled as springs with $k_y = 2.0 \cdot 10^7 \text{N/m}$ and $k_z = 1.0 \cdot 10^8 \text{N/m}$. The sleepers under the rails were restricted in z-direction.

	Lateral stiffness k_y	Vertical stiffness k_z
Ballast	–	$2.4 \cdot 10^7 \text{N/m}^2$
Railpads	$2.0 \cdot 10^7 \text{N/m}$	$1.0 \cdot 10^8 \text{N/m}$

Table 2.1: Material properties for ballast and railpads.

The bolts which connects rail and fishplate are modeled as rigid beams consisting of three nodes, one in each fishplate and with the center node in the rail. The bolt nodes can be seen in figure 2.2. The rigid bolt beams are allowed to rotate. A quasi-static approach was employed. For each time-step point loads representing the loads of one (or in some cases two) wheel sets were applied to the rails. At each time increment the load was moved one node forward, see figures 2.3 and 2.4. The resulting bending moments and sectional forces were analyzed in the post-processor Abaqus CAE. This analysis revealed the location of critical points both along the rail and regarding wheelset position(s).

2.1 Mesh influence

Since finite element solutions are numerical approximations, it is important to understand the related errors. To this end, a mesh convergence analysis was employed. As seen in figure 2.5 the results converge as the mesh size decreases. From the analysis a mesh with element lengths in the rail ranging from $0.0175m$ to $0.035m$ was deemed sufficiently dense.

The element type that was used in Abaqus to model the rail was B31. It is a 2-node linear beam in space that allows for transverse shear deformation according to Timoshenko beam theory.

	Rail	Sleeper section 1	Sleeper section 2	Sleeper section 3	Sleeper section 4	Sleeper section 5
Young's modulus, E (Pa)	$2.1 \cdot 10^{11}$	$4 \cdot 10^{10}$	$4 \cdot 10^{10}$	$4 \cdot 10^{10}$	$4 \cdot 10^{10}$	$4 \cdot 10^{10}$
Shear modulus, G (Pa)	$8.08 \cdot 10^{10}$	$1.74 \cdot 10^{10}$	$1.74 \cdot 10^{10}$	$1.74 \cdot 10^{10}$	$1.74 \cdot 10^{10}$	$1.74 \cdot 10^{10}$
Poisson's ratio, ν	0.3	0.15	0.15	0.15	0.15	0.15
Density, ρ (kg/m^3)	7800	2400	2400	2400	2400	2400
Cross-section area, A (m^2)	$6.37 \cdot 10^{-3}$	$4.71 \cdot 10^{-2}$	$4.83 \cdot 10^{-2}$	$4.46 \cdot 10^{-2}$	$3.78 \cdot 10^{-2}$	$3.32 \cdot 10^{-2}$
Area moment of inertia, I_{11} (m^4)	$20.5 \cdot 10^{-6}$	$1.69 \cdot 10^{-4}$	$1.81 \cdot 10^{-4}$	$1.67 \cdot 10^{-4}$	$1.18 \cdot 10^{-4}$	$8.98 \cdot 10^{-5}$
Area moment of inertia, I_{22} (m^4)	$3.37 \cdot 10^{-6}$	$2.54 \cdot 10^{-4}$	$2.75 \cdot 10^{-4}$	$2.16 \cdot 10^{-4}$	$1.31 \cdot 10^{-4}$	$8.92 \cdot 10^{-5}$
Transverse shear stiffness, kGA (N)	$2.06 \cdot 10^8$	$6.22 \cdot 10^8$	$6.37 \cdot 10^8$	$5.87 \cdot 10^8$	$4.98 \cdot 10^8$	$4.38 \cdot 10^8$

Table 2.2: Material properties for rail and sleeper beam elements. From [5]. The sleeper sectioning is shown in figure 2.1

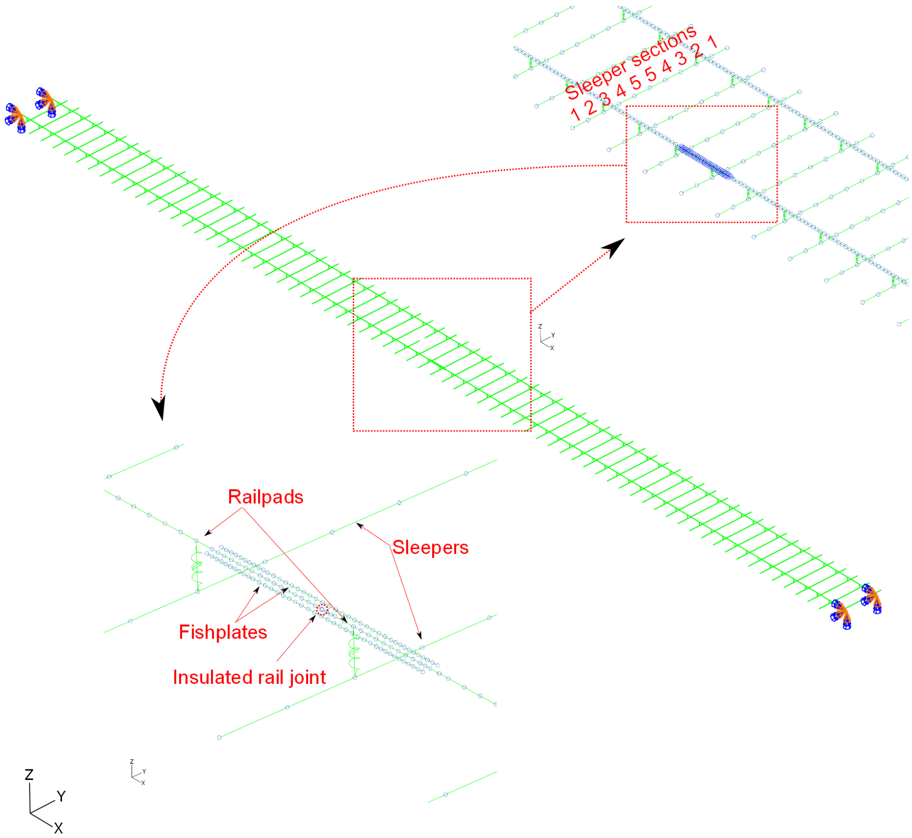

Figure 2.1: Illustration of the track model used in Abaqus simulations.

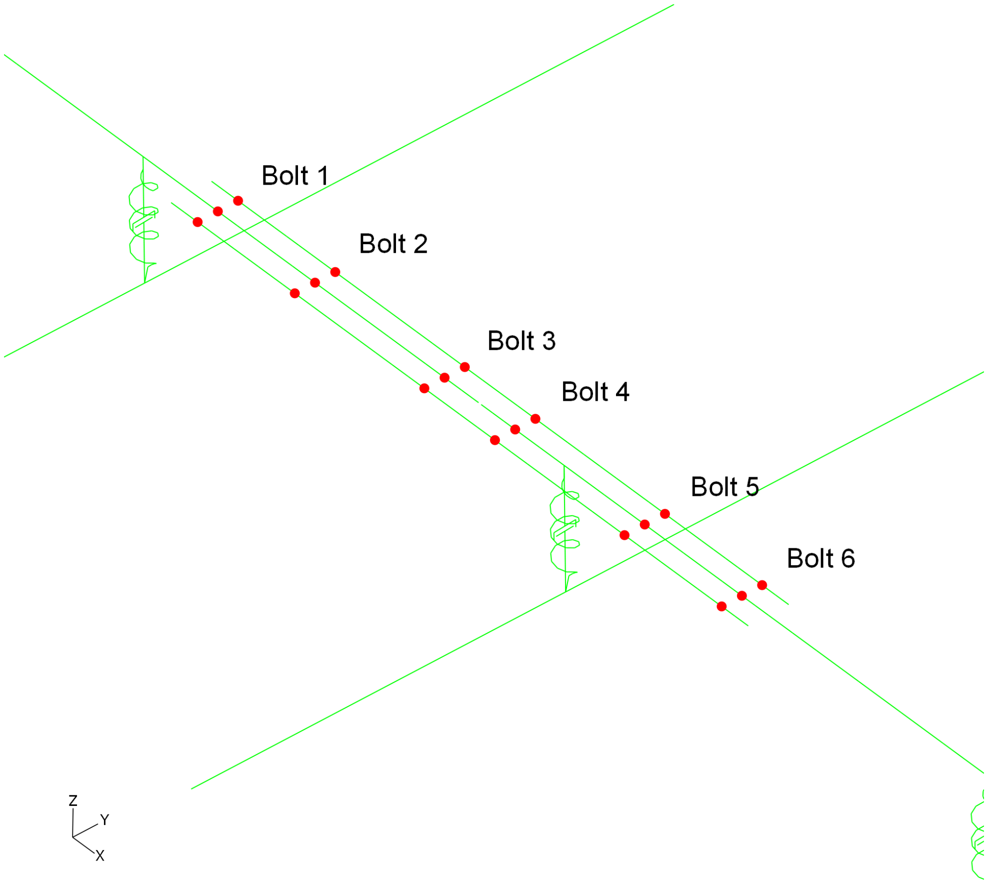

Figure 2.2: Location of bolt nodes used in the Abaqus model.

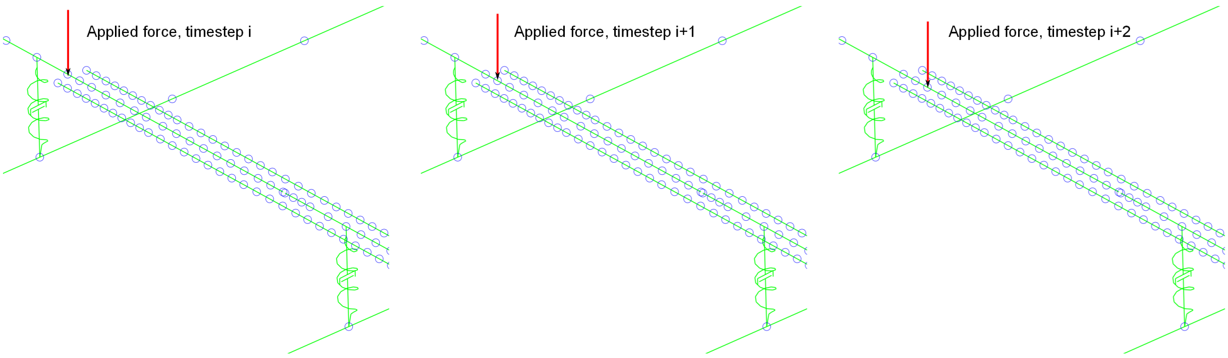

Figure 2.3: Zoomed in picture of rail 1 showing how the force is moved along the rail. An identical force with the same magnitude is applied on rail 2 (not shown in figure).

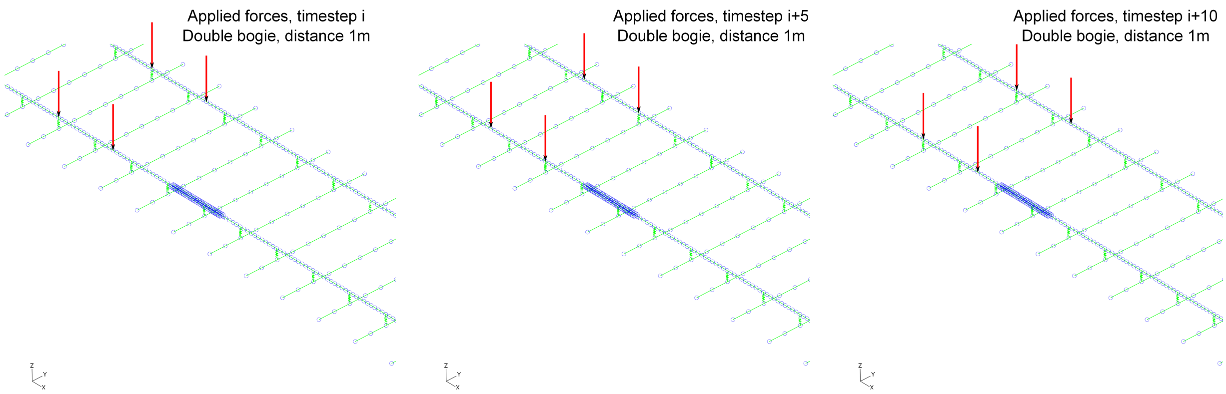

Figure 2.4: Illustration of the quasistatic approach in Abaqus for a bogie system with axle distance of 1 meter. There are five timesteps between each picture.

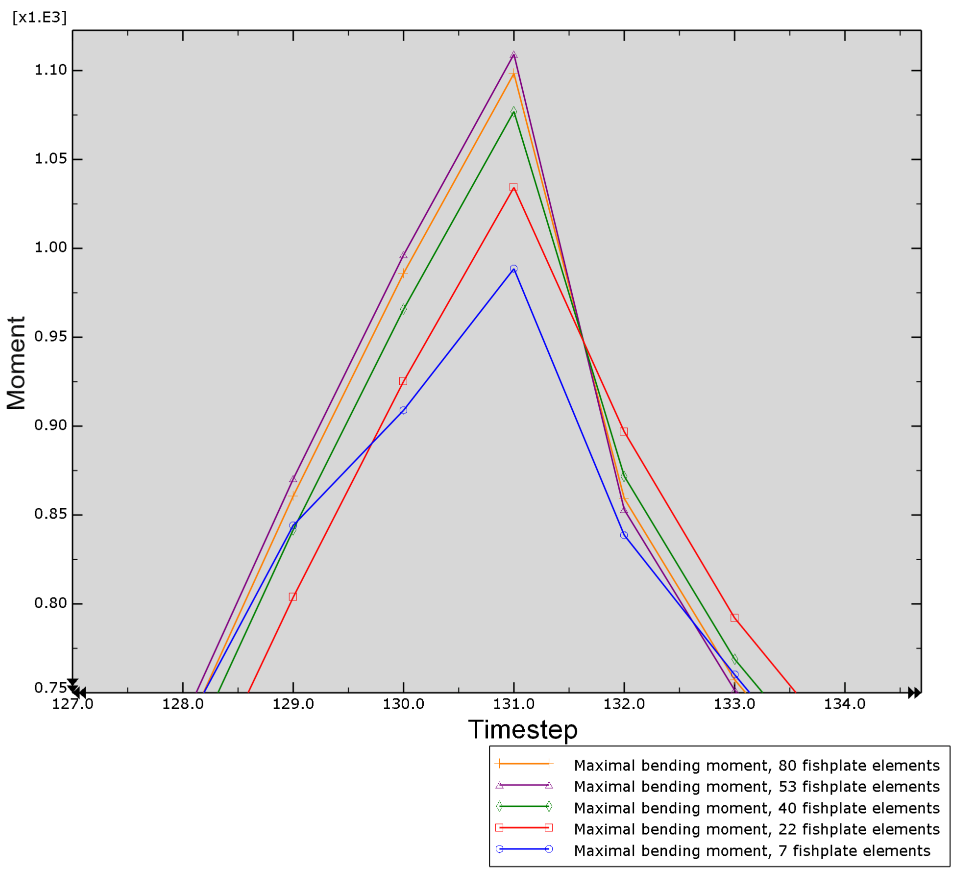

Figure 2.5: Maximum bending moment in fishplate given varying numbers of elements in the fishplate.

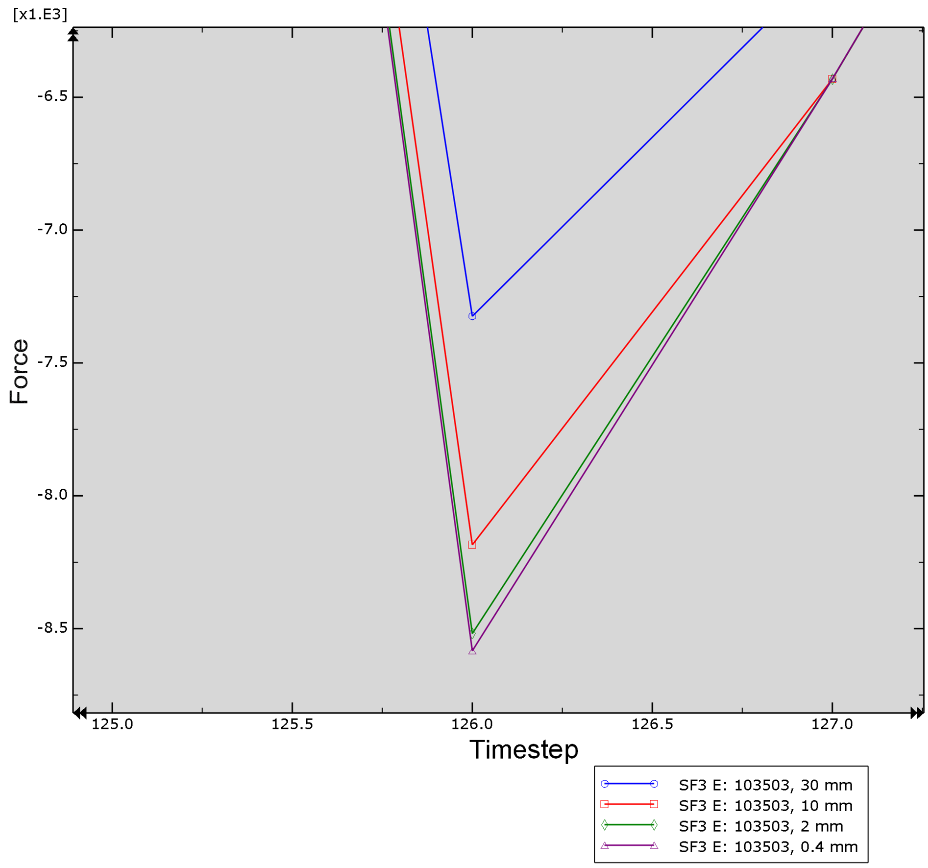

Figure 2.6: Force convergence in element closest to first bolt, applied example load 10kN.

The shortest element lengths in the rail have here been employed close to the bolts. Two kinds of mesh convergence checks were used. Firstly all element lengths were reduced to check if the response distribution was similar. The refinements indicate that the mesh is sufficiently dense to determine where the maxima are located.

Due to the refinement around the insulated joints, the element lengths are different in the two rails, which results in that the forces of the left and right wheel are not applied at exactly the same coordinates along the rail. This is however not a big problem since the force position on one rail does not have a major influence on the response in the other rail (the difference is less than 1%).

The mesh was thereafter refined in the regions where the responding forces were the highest. The reason to confine the refinement to this region was to save computational time since the response in the intermediate regions was of less interest, the objective of the study was to localize the maxima, not to determine the exact response in every point. In figure 2.6 one can see that the force maxima converges in the studied regions, with a magnitude of the shear force range equal to the applied load, as expected (see table 2.3).

2.2 Investigated parameters

It is important to identify the parameters deemed most influential for joint degradation. In this project the axle distance (see chapter 3.1), the rail profile (3.3) and joint position (3.4) have been investigated. Dynamical effects from speed of the train and direction of traffic have not been investigated but might be topics in follow-up projects.

Node distance at bolt 1	Maximal positive force	Maximal negative force	Force difference
30mm	1403N	−7325N	8728N
10mm	1403N	−8185N	9588N
2mm	1400N	−8518N	9918N
0.4mm	1400N	−8584N	9984N

Table 2.3: Force response in element closest to first bolt, applied example load 10kN.

3 Load modeling

In the simulations the loads acting on the rails have been applied as point loads in one node per rail at each instant in time. The point of application is then moved along the rail. Based on the result of the convergence study (see chapter 2.1) the nodes are placed at a minimal distance of 17.5mm. Since the length of the actual contact pressure distribution in the wheel-rail contact in practice could be at most some 30mm, and we are not evaluating the contact stress field but the bending moment in the rail, it is a reasonable simplification to adopt point loads in the quasi-static simulation.

3.1 Single and double axle bogies

To evaluate the influence of the nearby wheelset in a bogie, and thus assess whether the bogie distance is of interest in the calculations, simulations with two different axle distances were carried out. The bogie load was modeled as four point loads (two on each rail). These loads were then moved one node in each simulation increment, an illustration of the procedure is shown in figure 2.4.

As can be seen in figure 3.1 the difference between the single bogie model and the double bogie models is somewhat influenced by the different bogie distances. For distances of 3 meters the maximum negative moment becomes larger and the maximum positive bending moment is almost identical to the single bogie situation. For an axle distance of 1 meter the cycles interact so that the minimal bending moment between the positive peaks is positive. If the rail profile is changed, the bending moment magnitude changes (see figure 3.2) and hence also the effects of bogie distance.

Dynamic effects related to the different bogie distances might be larger. However, dynamic effects are not considered in this study due to the complexity they include that basically makes any attempt at standardization futile, see further chapter 3.2.

Additionally, the aim of the project is to develop a standard for comparison between different insulated joint constructions subjected to loads that reflect the operational conditions. It is therefore not a primary concern to account for minor deviations due to the bogie construction, the main focus is to establish sufficiently realistic load scenarios under which the different joints can be tested and compared. The actual load conditions will then vary depending on axle loads and speed (due to dynamic effects), bogie distances, support conditions etc.

Bogie distances affect the response, but it does not change the location of the critical points.

Since the maximal moment is similar in all situations studied the conclusion from this part of the investigation was to carry out the tests with loads corresponding to a single axle load system.

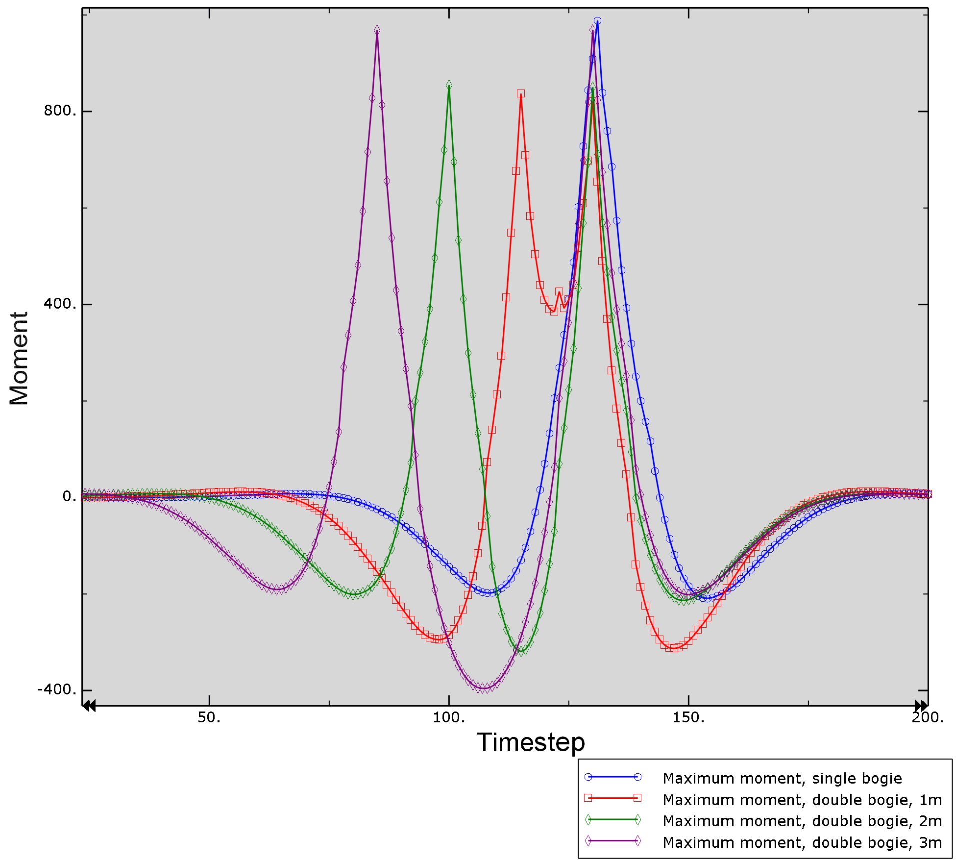

Figure 3.1: Bending moments for single and double bogie with axle distances of 1, 2 and 3 meters.

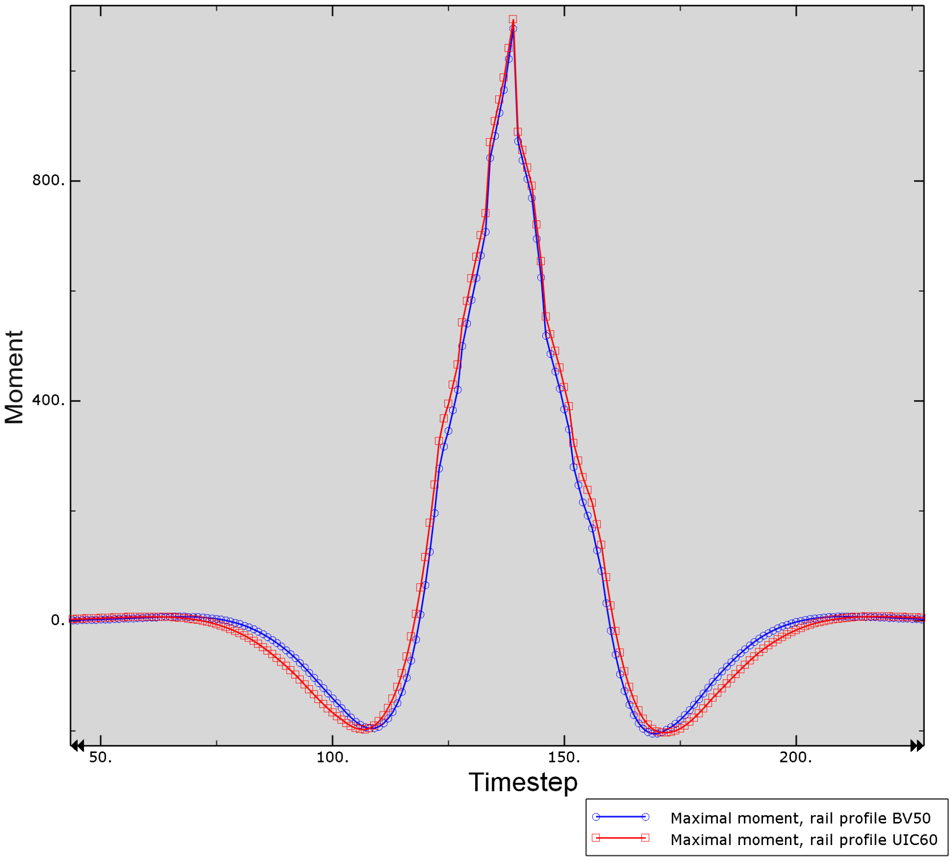

Figure 3.2: Bending moments for rail profiles UIC60 and BV50.

3.2 Dynamic load effects

The loading generated by a moving vehicle on a rail can be divided into a (quasi-) static and a dynamic contribution. The latter is governed by the dynamic response of the system and influenced by parameters such as vehicle speed, sleeper spacing, dynamic properties of suspension etc. Thus, the dynamic contribution is strongly related to the operational characteristics of the passing vehicles and also the rail foundation (sleepers, ballast etc). However, the aim of the current study is not to evaluate the loading of an insulated joint as accurately as possible, but rather to design a sufficiently realistic test set-up in which different insulated joints can be tested. For this reason, an analysis of the dynamic effects has been excluded from the current study. This does of course not mean that insulated joints are not subjected to dynamic load effects. These may exist and may be significant, especially for run-down joints (see [5]). However they can be approximated by an increase in the applied static load magnitude.

It also does not mean that the dynamic load effects are the same for all insulated joints. They may vary depending on the design of the joint. This influence can be assessed in a separate analysis of the dynamical characteristics of the joint: The recommended test set-up (see 3.6) includes a step-increase of the applied loads. If one wants to roughly evaluate the effects of dynamical load contributions, one could thus evaluate the response at a higher load magnitude.

3.3 Rail profile

In Sweden, the two most frequently used rail profiles are UIC60 (60E1) and BV50 (50E3) (see figures 7.1, 7.2, 7.3 and 7.4). Simulations have been carried out to compare the resulting bending moments and sectional forces in the joint components given the different rail profiles. As can be seen in figure 3.2 the results differ little between the two profiles regarding maximum bending moments, but somewhat more regarding the response distribution, which can be of interest if a double axle bogie model is used. In this project, as mentioned before, double axle bogie effects are not treated and therefore the difference between the rail profiles is sufficiently small to be neglected in further calculations. Consequently, if nothing else is stated, the BV50 profile is employed and analyzed below.

If for some reason more exact calibrations are needed, different test setups could be used for different rail profiles. However, as discussed above – the main aim is to establish sufficiently realistic test conditions that make tests of different joints comparable, not to exactly model the real situations.

3.4 Joint position

There are basically two philosophies of how the insulated joint shall be positioned, as shown in figure 3.3. When the joint is placed in the center of a sleeper span, the highest shear force in the full-scale model is found in bolt 2. It would however be desirable to have a testing procedure that is applicable for both positions of the joints. Since the material structure of the rail should be the same around both bolt 1 and 2 (the rail and fishplate profiles are of same shapes, but the boundary conditions differs) it would be sufficient to just measure on bolt 1 in the test even if it would be bolt 2 that gets the highest stress. In addition from a testing perspective it is easier to apply loads further apart from each other, to apply loads on bolt 2 and over the area around the insulating material might be too difficult to carry out.

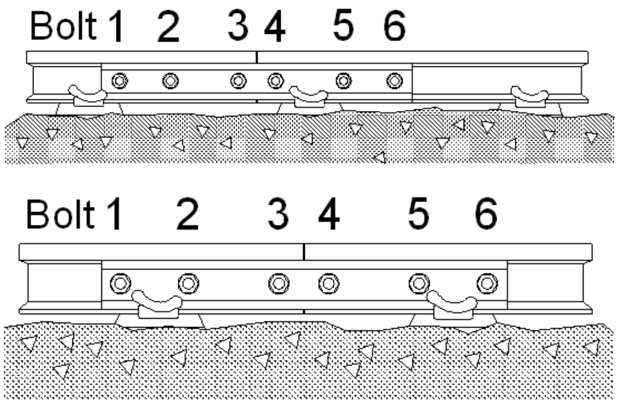

Figure 3.3: Two common positions of the insulating joint relative to nearby sleepers.

3.5 Insulation material

Results from the literature [5] conclude that very limited amounts of the applied load is carried by the insulating material. Consequently, the insulation layer is numerically modeled as a gap in the current simulations. This simplification should have very small effect on the results since the elastic modulus of the joint is very low compared to that of the rail ($2.5 \cdot 10^9$ and $2.1 \cdot 10^{11}$N/m^2, respectively).

3.6 Test specimen

The next step in developing a test set-up was to recommend a length of the test specimen. In addition it was important to conclude which load scheme that should be recommended, and which boundary conditions that would be feasible.

The boundary conditions were chosen as simply supported. The main reason was that it would require very high clamping forces in the rail ends to maintain the beam inclination and therefore it would have been difficult to make the tests reproducible and cost-effective.

To make it possible to accomplish the tests in as many labs as possible a goal was to reduce the length of the beam. The evaluation of a feasible beam length was based on an analysis of where in the model the maximum force and the maximum bending moment arise. The next step would therefore be to design the test specimen such that the response in the critical points would be as similar to the "reality" as possible.

Instead of applying the load as a rolling wheel, which would have been both expensive and inexact, the applied load was chosen as two point loads, one in each of the selected critical points (see figure 4.3). It is important that the load functions are not designed in such way that the force and moment responses result in additional load cycles (see figure 4.2). Except from that restriction, the time evolution of the loads is of less importance. According to fatigue design theory [2] the number of cycles to failure is related only to the maximum and mean load magnitude.

The loads are scaled such that the response (in terms of bending moment and shear force magnitude) corresponded to the complete rail structure. The reason why the two loads are not scaled equally is that the point of application vary and thereby are differently affected by the boundary conditions.

Since the shear force and bending moment ratios (min value divided by max value) differ between the full-scale rail structure and the test set-up, this needs to be compensated for.

	Maximum	Minimum	Equivalent maximum	Quotient
Force in rail at bolt 1	−8600N	1400N	9270N	1.078
Bending moment in fish-plate near joint	1077Nm	−195Nm	1170Nm	1.086

Table 3.1: Maximum and minimum force at bolt and moment at joint for an applied force of 10kN in the quasistatic FE simulation. From these magnitudes the equivalent maxima according to the Smith–Watson–Topper [4] criteria are calculated. Since the model is linear it is possible to scale the above values to desired level. The quotient is computed as Equivalent maximum/maximum.

To this end the Smith–Watson–Topper [4] criteria has been employed to evaluate equivalent forces and bending moments, see table 3.1.

There should be no complications related to the fact that the specimen only is loaded in two points and that measurements are made at two locations. This is because of the assumption that the areas around the bolts are assumed to behave in the same way and therefore it is only important to apply load and measure the response in the most critical point. It is important to ensure that the selected critical points are indeed the highest stressed.

3.7 Error margins

If the test specimen length is for some reason longer or shorter than proposed or if the loads are applied on other locations, it is important to predict if the structure behaves in another way than if it is properly done. If the distance between the supports is increased with 0.01m in each end, the maximum bending moment is increased with less than 2% and if the beam length is decreased with 0.01m in each end the maximum bending moment decreased with less than 2%. See figure 3.4.

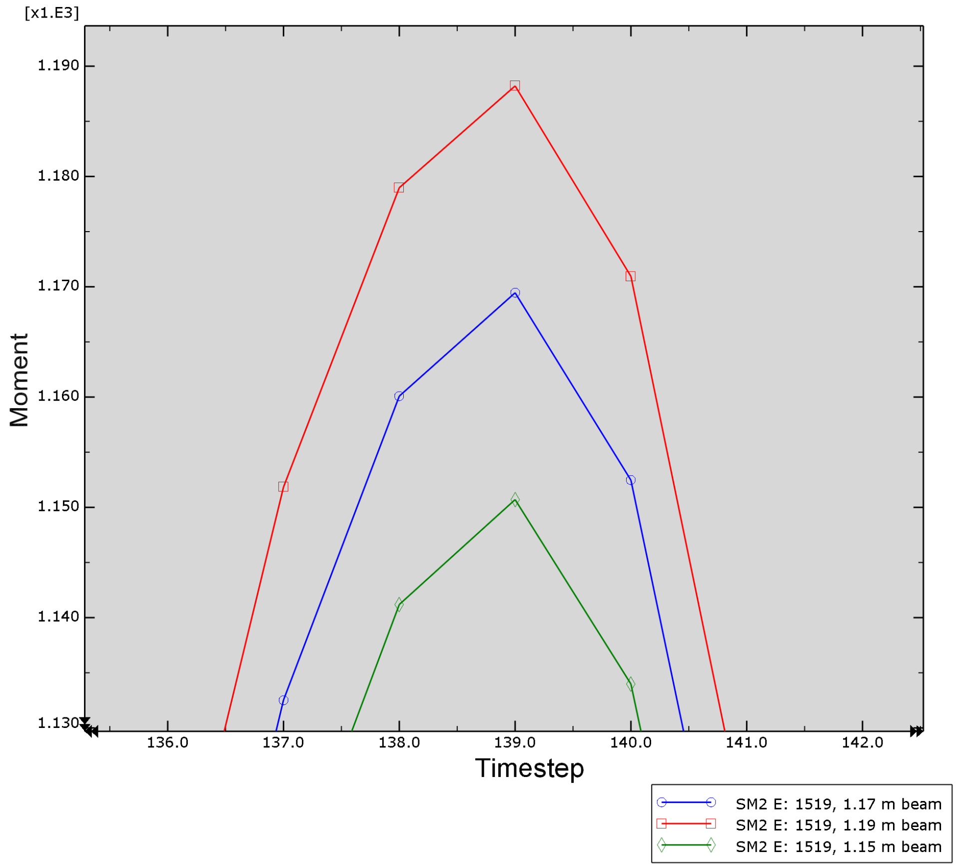

Figure 3.4: Maximum bendin moment in test specimen for different lengths given an equivalent static force of $10kN$.

4 Test setup

In Abaqus, a test specimen was modeled on which forces were applied in two points, see figure 4.3. The aim is to get a similar force-response in the region close to bolt 1 and a similar bending moment response in the region around the joint for the test specimen model as compared to the quasi-static track model. To achieve this, two forces were applied, one over bolt 1 and one over the joint. To model a situation similar to the quasi-static one the forces are to be applied as sinus-shaped waves as can be seen in figure 4.1 b), i.e. with a phase shift of half a period. The load on the joint starts when the load is maximum at bolt 1, and the load on bolt 1 reaches zero when the load is maximum at the joint.

In addition the set-up with two forces makes it less favorable to optimize only towards better strength in one region (e.g. around the joint material / center of the fishplates).

4.1 Test procedure

The recommended test procedure is as follows: First the test is done with loads equivalent to 25 tonnes axle load for 200 000 cycles, thereafter the load is increased with steps equivalent to 5 tonnes for 100 000 cycles each, see table 4.1. When the equivalent load has reached 50 tonnes the test is run until breakage, or at most an additional 500 000 cycles.

Since the fatigue strength is independent of loading frequency and since the eigenfrequency of the beam was computed to be around 197Hz which is much greater than what is feasible in a laboratory, the frequency of the test can be chosen arbitrary. It is important that the frequencies of the two loading cycles are the same and that a phase shift as in figure 4.1 b) is adopted.

Between each change of load magnitude, photographes are to be taken to make it possible to determine the specimen deterioration before break. Required photos are listed below.

Photographes to be taken between each load cycle:

1. From one side, perpendicular to the rail, at the joint
2. From the other side, perpendicular to the rail, at the joint
3. From one side, perpendicular to the rail, at bolt 1
4. From the other side, perpendicular to the rail, at bolt 1
5. From above on the joint
6. From below on the joint
7. From above on the point where the load is applied over bolt 1
8. From below the rail under bolt 1

Summary of load instructions:

1. At each increase in load magnitude the standardized electrical insulation test [7] shall be done
2. Before the load cycles are started the given load on the joint shall be applied statically so that it is possible to measure the statical deformation of the rail.
3. The load cycles shall be sinus-shaped and pulsating (maxima equal to the double the amplitude)

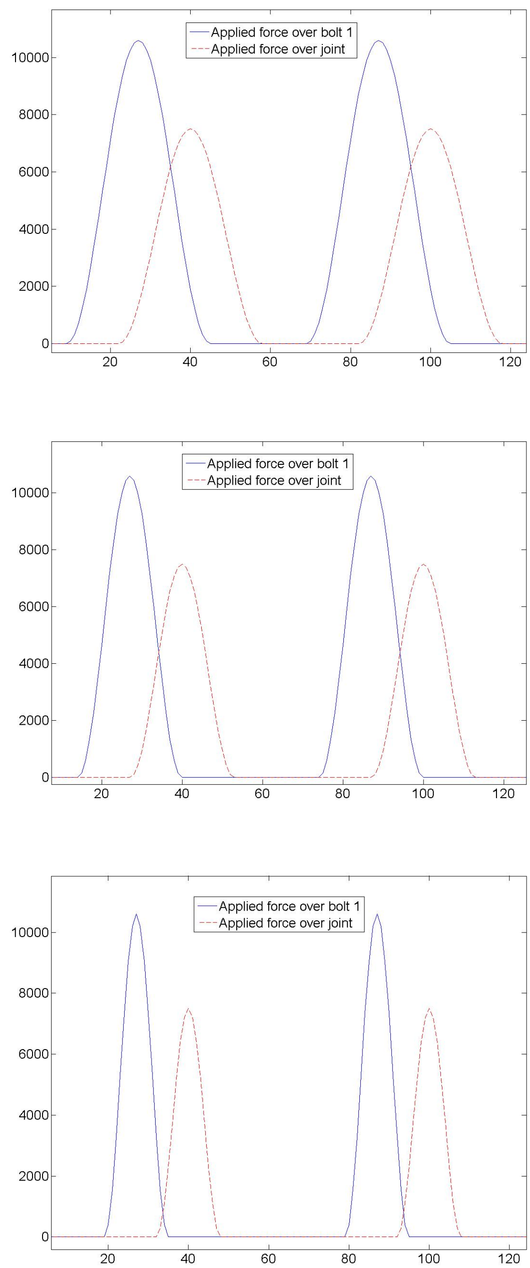

Figure 4.1: Three different phase shift profiles with phase shift of 0.36, 0.5 and 0.81 of the period time, respectively. Figure 4.2 shows the bending moment response given the different phase shifts.

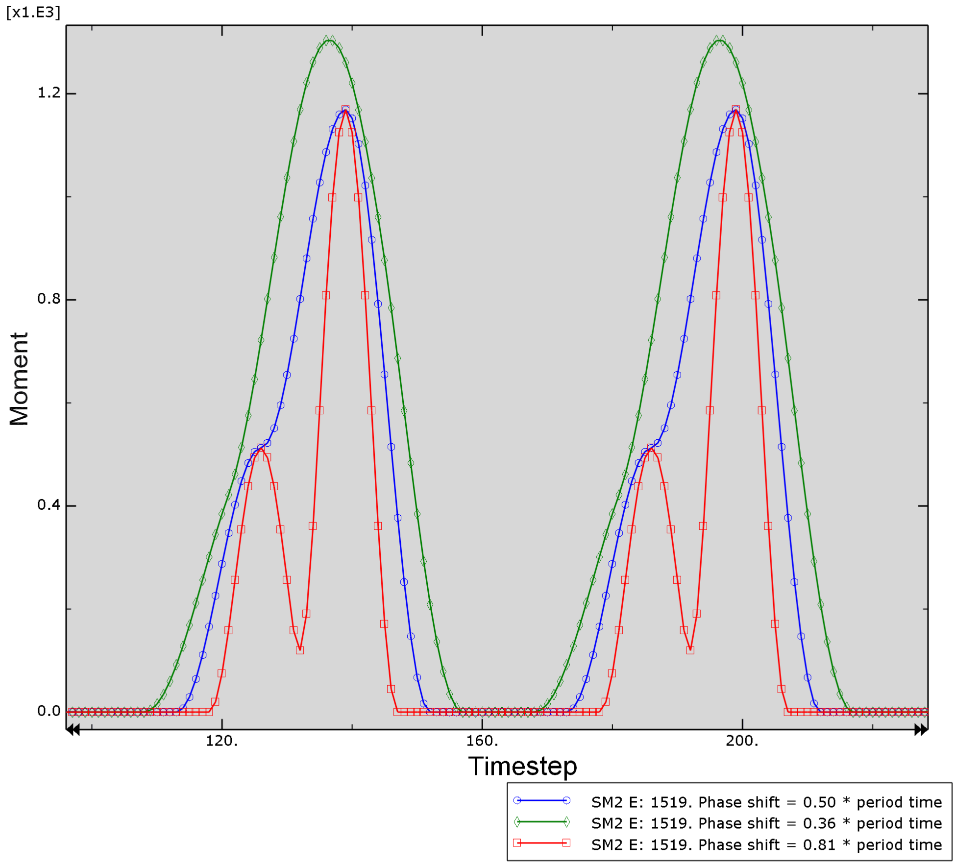

Figure 4.2: Bending moment response given the different phase shifts shown in figure 4.1. Too small phase shift (green rhombus line) gives too high bending moment response. If the phase shift is too large (red quadrat line) the bending moment response will contain additional load, which shorten the lifetime of the test specimen. Recommended phase shift is half of the period time, which in this figure is represented by the blue line with circles.

Equivalent axle load (tonnes)	Force over bolt 1 (N)	Force over joint (N)	Number of cycles
25	$1.23 \cdot 10^5$	$1.34 \cdot 10^5$	200 000
30	$1.47 \cdot 10^5$	$1.61 \cdot 10^5$	100 000
35	$1.72 \cdot 10^5$	$1.87 \cdot 10^5$	100 000
40	$1.96 \cdot 10^5$	$2.14 \cdot 10^5$	100 000
45	$2.21 \cdot 10^5$	$2.41 \cdot 10^5$	100 000
50	$2.46 \cdot 10^5$	$2.68 \cdot 10^5$	500 000*

* The structure will probably break before reaching 500 000 cycles at this level, so it shall be seen as an upper limit.

Table 4.1: Table of recommended load scheme.

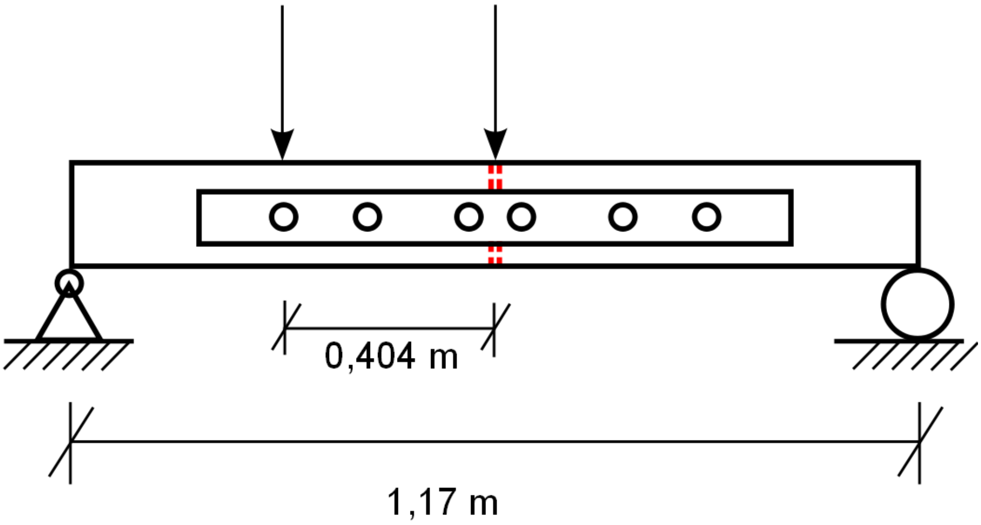

Figure 4.3: Recommended test set-up for test specimen of profile BV50.

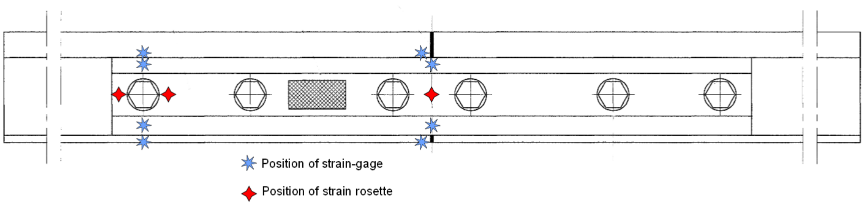

Figure 4.4: Recommended positions for strain-gauges and strain rosettes. See also figure 4.5

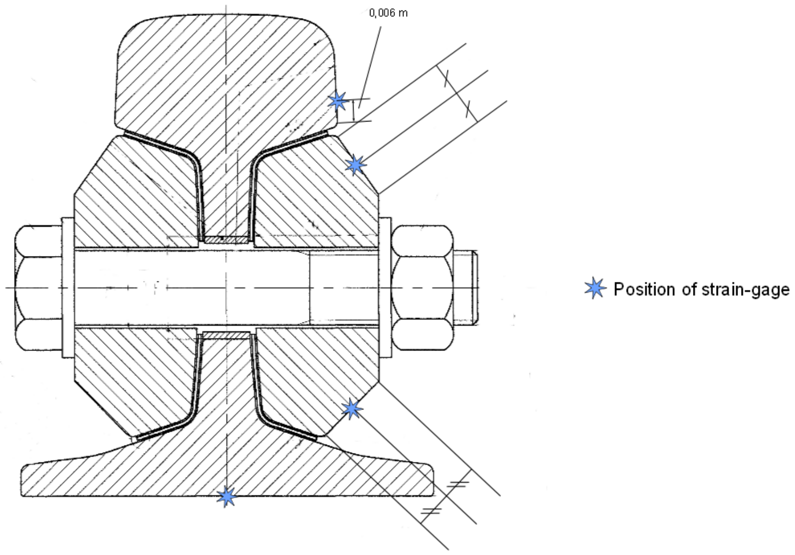

Figure 4.5: Recommended positions for strain-gauge in profile view. See also figure 4.4

4. The load cycles over bolt and joint shall have the same period length
5. The load applied over the joint shall have half a period phase shift as compared to the load applied over the bolt. First when the load over the joint has reached zero a new load cycle shall begin over the bolt. This means that there is at least half a period between the pulses. See figure 4.1 b.

5 Evaluation of field validation tests

To conclude which type of insulated joint that gives the least amount of operational disruptions (signalling errors) and the longest operational life-times statistical data have to be compared.

When comparing different types of joints one type is considered as the reference (usually the model already in use) with which an alternative is compared. In the model presented here the different types of joints (e.g. two types – with 4mm and 6mm gaps) are treated as two error-generating sources. Errors are here presumed as occur according to a Poission process. The joints are not compared individually; it would be too difficult to measure the performance of separate joints. Instead the two groups of joints (reference and "new") are compared. The comparison presumes that the groups are similarly affected from the surrounding environment. It is therefore important that the joints to be compared are installed at the same time (and thus in different places) instead of comparing with the joints that were placed at the same locations before. The reason is that both the joints and the track degrade over time. In addition, operational conditions, such as tonnage, vehicle types and climate may change. Thus if the joints are not installed at the same time, any comparison is very cumbersome. In particular comparing joints of different age will be very misleading.

To compare the joints one option is to sort the joints into so called twin tests. This implies that one combines the joints two and two such that each pair of joints (containing one "reference" and one "new" joint) has as equal surrounding and operational conditions as possible. To conclude if there are any statistically significant differences between the two joint types the difference in error occurrence for each pair is used as the stochastic variable. Although this is a very "clean" approach, it would probably be too difficult since it is not obvious how to sort into similar joint configurations (average speed of passing trains, average load, distance to station, frequency of passing trains etc).

The most practical way might instead be to randomly place the different joint types to make all external disturbances as evenly distributed as possible between the two joint groups. The randomness can be achieved as follows: First one determines all places where the joints shall be installed and the proportion of the two joint types (equal numbers of each type is not necessary but it makes the comparison easier). Then one randomizes which type of joint that shall be installed for each position. This procedure makes the external effects evenly spread from a statistical point of view and therefore the test more reliable.

The individual joints are not separately compared; instead the two types of joints are treated as two independent entities. The occurrence of errors are expected to be Poisson distributed and the evaluation of the test is done by constructing a confidence interval for the quotient of the failure intensities.

Here it should be noted that it is probably too difficult to carry out the analysis for a subdivision into different types of errors in the comparison. If deemed interesting, a separate study can instead be made to establish whether the dominating error types vary between the different joint types.

5.1 Determining which joint type that has the highest quality

To conclude if one of the joint types is more likely to generate errors, and therefore should be avoided, one formulates a null hypothesis that $\lambda_1 = \lambda_2$, where $\lambda_1 = \lambda_2$ are the Poisson intensities for joints of type 1 and 2, respectively. If one can determine that the null hypothesis is false within a given confidence interval one concludes that there are statistically

Confidence interval	Values for $\chi^2(1)_c$
90%	2.706
95%	3.841
99%	6.635

Table 5.1: χ^2-values for given confidence intervals. For a more detailed table, see [3]

significant differences in the failure probabilities. Following formula is then used [8]:

$$H_0: \quad \lambda_1 = \lambda_2 \tag{5.1}$$

$$\begin{aligned} Q &= \frac{(n_1+n_2)^2}{n_1 n_2 (x_1+x_2)} \left(x_1 - \frac{n_1(x_1+x_2)}{n_1+n_2} \right)^2 = \\ &= \frac{(n_1+n_2)^2}{n_1 n_2 (x_1+x_2)} \left(\frac{n_2 x_1 - n_1 x_2}{n_1+n_2} \right)^2 = \\ &= \frac{(n_2 x_1 - n_1 x_2)^2}{n_1 n_2 (x_1+x_2)} \end{aligned} \tag{5.2}$$

$$Q(n_1 = n_2) = \frac{(x_1 - x_2)^2}{x_1 + x_2} \tag{5.3}$$

λ_1	Poisson intensity for joint type 1
λ_2	Poisson intensity for joint type 2
n_1	Number of joints of type 1
n_2	Number of joints of type 2
x_1	Number of errors generated by joint type 1 during the test period
x_2	Number of errors generated by joint type 2 during the test period
x_{2c}	Required value of x_2 to achieve a given confidence interval c
$\chi^2(1)_c$	Value depending on given confidence interval, see table 5.1

If Q exceeds the prescribed values in column 2 of table 5.1 then the null hypothesis is false within a confidence interval of the value in column 1 on the corresponding row. The χ^2-distribution is used since a division of Poisson variables is used and the degree of freedom of 1 is equal to the number of compared types minus 1 (one). To calculate the required value x_{2c} to achieve a confidence interval c for a given value of x_1 the following formula is used, given $n_1 = n_2$:

$$\begin{aligned} \frac{(x_1 - x_{2c})^2}{x_1 + x_{2c}} &> \chi^2(1)_c \\ x_{2c}^2 - x_2\chi^2(1)_c - 2x_1 x_{2c} &> x_1\chi^2(1)_c - x_1^2 \\ \left(x_{2c} - \left(\tfrac{1}{2}\chi^2(1)_c + x_1\right)\right) &> x_1\chi^2(1)_c - x_1^2 + \left(\tfrac{1}{2}\chi^2(1)_c + x_1\right)^2 \\ x_{2c}^2 &> \tfrac{1}{2}\chi^2(1)_c + x_1 + \sqrt{x_1\chi^2(1)_c - x_1^2 + \left(\tfrac{1}{2}\chi^2(1)_c + x_1\right)^2} \end{aligned} \tag{5.4}$$

The formula shows greater significance the larger x_1 and x_2 are given same quota between the numbers. Analogous to this the required quotient of x_1 and x_2 is lower the larger the numbers become. For example, if $n_1 = n_2$, $x_1 = 10$, x_2 has to be 21 or higher to assure a 95% confidence interval for $x_2 > x_1$. If $x_1 = 100$ then x_2 has to be 130 for the same confidence interval. This indicates that the higher the number of failures, the more significant results can be obtained in determining which of the two joint types that is more probable to generate errors.

It is possible to make more than one comparison, for example if one wants to know if a special type of insulated joint is more suitable for a specific situation. One should however be careful not to divide the evaluation test into too small groups. As can be seen in table 5.2 if one of the joints has generated 10 errors during the test period and the other one twice as many (20) errors you do not even have a 95% confidence interval that the first joint is of higher quality. If you instead let the test run over a longer period of time and/or include more joints in the test so that one of the joint types generates 100 errors you can, within a 99% confidence interval conclude that this joint is of higher quality than the other if the other one has generated twice as many (200) errors during the test period. Longer time intervals and more tested joints gives more robust conclusions as to whether one of the joints is more reliable than the other.

It is however possible, and recommendable to both compare error statistics on the whole and error statistics for different parts of the validation study to identify any anomalies (e.g., an excessive number of errors for a certain joint) that may not be related to the joint type in itself.

Conclusions for obtaining a high significance in validation testing:

- Remove external variables by randomizing the placement of the joints.
- Compare as few types of joints as possible, preferably only two types.
- Install the joints at same time to remove effects of weather, change in traffic etc.
- Include as many joints as economically and operationally possible – the more joints, the higher the significance of the test.
- Let the test continue over a long period of time, the longer the better. Preferably the test should continue until all joints have reached their operational life and are replaced or subjected to excessive revision. It might be that one type of joint is better in the short perspective in the sense that it generates less errors but instead has a shorter life-time. The results of such an analysis together with an analysis of which joint type that is to be preferred – one with a long life-time or one with few operational errors – should form the decision for which joint type to adopt under a given operational condition.
- Be sure to relate operational errors to the correct joint. If this cannot be done, the reliability in the evaluation is reduced.
- File the errors so that it can be possible after the tests to determine if special types of joints are more suited for special locations etc. If possible, classify the error.

5.2 Quality factor comparison

The method above is not applicable to determine how big the difference is in quality between the two types of joints, only to determine if you with a given confidence interval can conclude if one of the joints is less error prone than the other. To evaluate the actual difference in quality could be of interest if the prices of the two joints are different and one needs to know if it is worth the higher price to reduce errors. For such a comparison, the following methodology is used [8]:

	Least number of x_2 to achieve given confidence interval		
x_1	90%	95%	99%
10	19	21	26
20	32	35	40
50	68	72	80
100	125	130	140
200	235	242	256
500	554	564	586
1000	1075	1090	1119

Table 5.2: Table of number of recorded errors required to achieve confidence intervals for determining which joint that is of highest quality.

$$H_0: \quad f \cdot \lambda_1 = \lambda_2 \tag{5.5}$$

$$Q = \frac{(fx_1 - x_2)^2}{(x_1 + x_2)} \tag{5.6}$$

Where f is the factor of how much more erroneous the joint that has generated the highest amount of errors is as compared to the other joint type. If f is 1.5 it means that the more erroneous joint in average generates 50% more errors than the less erroneous joint. Then the following equations are used to determine the least required value of x_{2cf}

$$\begin{aligned} \frac{(fx_1 - x_{2cf})^2}{f(x_1 + x_{2cf})} &> \chi^2(1)_c \\ x_{2cf}^2 - fx_2\chi^2(1)_c - 2fx_1x_{2cf} &> fx_1\chi^2(1)_c - f^2x_1^2 \\ \left(x_{2cf} - \left(\tfrac{1}{2}f\chi^2(1)_c + fx_1\right)\right)^2 &> fx_1\chi^2(1)_c - f^2x_1^2 + \left(\tfrac{1}{2}f\chi^2(1)_c + fx_1\right)^2 \\ x_{2cf}^2 &> \tfrac{1}{2}f\chi^2(1)_c + fx_1 + \sqrt{fx_1\chi^2(1)_c - f^2x_1^2 + \left(\tfrac{1}{2}f\chi^2(1)_c + fx_1\right)^2} \end{aligned} \tag{5.7}$$

f	Quality factor, see table 5.3
x_{2cf}	Required number of x_2 to achieve given confidence interval c if the quality factor is set to f

In table 5.3 f-values of 1.1, 1.25 and 1.5 are used. If Q is higher than corresponding $\chi^2(1)_c$-value one can reject H_0 within a significance interval given by c. Some pre-calculated values are given in table 5.3.

> Example: Assume that you have two types of joints and one of the joint types ($joint_1$) has generated 100 errors during the test period. If the other joint type ($joint_2$) has generated 145 errors during the same time period (which is $\geq$ 142, see row 6, column 2 in table 5.3) errors during the same time period you can conclude within a 95% confidence interval that λ_2 (the error density variable of $joint_2$) is at least 10% higher than λ_1. If x_2 instead should have been 194 ($\geq$ 191, see row 6, column 6) you would have had a 95% confidence interval that λ_2 is at least 50% higher than λ_1.

λ_2/λ_1	> 1.1		> 1.25		> 1.5	
x_1	95%	99%	95%	99%	95%	99%
10	23	28	26	31	31	37
20	41	48	43	49	51	58
50	79	88	89	98	105	116
100	142	153	161	173	191	206
200	265	280	299	316	357	376
500	619	642	701	726	838	867
1000	1197	1228	1357	1391	1623	1663

Table 5.3: Values for x_2 required to achieve different confidence intervals for different quotients of λ_2/λ_1. Calculated by equation 5.7

Normal distribution	
Confidence interval c	a_c
90%	1.282
95%	1.645
99%	2.326

Table 5.4: Values for normal distribution parameter a_c for different confidence intervals.

5.3 Mean life estimation

After the last joint has been replaced or been extensively revised it is possible to compare the mean operational life of the two joint types. Here the two types are denoted x and y. To evaluate the confidence interval, the mean operational life is approximated as being Normal distributed, see e.g. [1].

The joint with highest mean operational life during the test is denoted x. The lifetimes of the individual test joints are denoted $x_i, i = 1, ..., n$ and $y_j, j = 1, ..., m$. From these, mean values $\bar{x}$ and $\bar{y}$ and variances s_x^2 and s_y^2 are calculated as:

$$\begin{aligned}
\bar{x} &= \sum_{i=1}^{n} \frac{x_i}{n} \\
\bar{y} &= \sum_{i=1}^{n} \frac{y_i}{m} \\
s_x^2 &= \sum (x_i - \bar{x})^2/(n-1) \\
s_y^2 &= \sum (y_i - \bar{y})^2/(m-1)
\end{aligned} \tag{5.8}$$

Finally one can construct a confidence interval for the difference of the two expected mean life times μ_x and μ_y. μ_x is greater than μ_y within a confidence interval of c if the following inequality holds [6]:

$$\bar{x} - \bar{y} - a_c \cdot \sqrt{\frac{s_x^2}{n} + \frac{s_y^2}{m}} \geq 0 \tag{5.9}$$

Where a_c is related to the Normal distribution as given in table 5.4.

5.3.1 Mean life time estimation, five joints of each type

Assume that there are 5 joints of type 1 and 5 of type 2 (n=5, m=5). The lifetimes are listed in table 5.5.

Type1	Type2
5	4
6	5
7	6
8	7
9	8

Table 5.5: Lifetimes in years for two joint types.

$\bar{x}_1 = 7, \bar{x}_2 = 6$ Assume null hypothesis H_0 that $\mu_1 = \mu_2$ Given 95% confidence, $\mu_x - \mu_y$ is at least

$$\begin{aligned} \bar{x} - \bar{y} - a_{0.95} \cdot \sqrt{\frac{s_x^2}{n} + \frac{s_y^2}{m}} = \\ = 7 - 6 - 1.645 \cdot \sqrt{\frac{2.5}{5} + \frac{2.5}{5}} = \\ 1 - 1.645 \cdot 1 = -0.645 \end{aligned} \tag{5.10}$$

and since this value is not equal or greater than 0 the null hypothesis cannot be rejected. That means that we cannot with 95% certainity say that type 1 on average has a longer operational life-time than type 2.

5.3.2 Mean life time estimation, 15 joints of each type

Assume instead that there are three times as many joints of each type, and that the lifetimes are distributed similar to the previous example. Life time distribution in this example is given in table 5.6.

For the same confidence interval as before (95%) $\mu_x - \mu_y$ is at least

$$\begin{aligned} \bar{x} - \bar{y} - a_{0.95} \cdot \sqrt{\frac{s_x^2}{n} + \frac{s_y^2}{m}} = \\ = 7 - 6 - 1.645 \cdot \sqrt{\frac{2.143}{15} + \frac{2.143}{15}} = \\ = 1 - 1.645 \cdot 0.535 = 0.121 \end{aligned} \tag{5.11}$$

since this value is greater than 0 the null hypothesis can be rejected within a 95% confidence interval, that is we can with 95% certainity say that type 1 on average has a longer operational life-time than type 2. This exemplifies how you can get more significant results if you have more test objects.

5.4 Some simplifications and assumptions made in the above study

Failure intensity is treated as constant over time. This assumption is made since no pre-knowledge exists on how failure intensities evolves over time. Failure intensity is also

Type1	Type2
5	4
5	4
5	4
6	5
6	5
6	5
7	6
7	6
7	6
8	7
8	7
8	7
9	8
9	8
9	8

Table 5.6: Lifetimes in years.

treated as unchanged by reparations. This is connected to the simplification that all kind of errors are treated equally in the statistics evaluation, and therefore it is not possible to include altered failure intensities after repair. No consideration is made regarding influencing effects. However if the joints are randomly placed so that they on average are equally affected this should be no problem as discussed above.

6 Concluding remarks

6.1 Laboratory test set-up

It is important and inquired to have a standard for bending tests of insulated joints which makes it possible to compare different types of joints. This project is a step in that direction. The recommended test beam of length 1.17m should be sufficient to evaluate the performance of different insulated joints under operational loading. Due to the relatively short length and simple boundary conditions, the test arrangement should be easy to accomplish.

6.2 Validation tests

The statistical methods oulined in this report should be applicable in different comparisons, not only for insulated joints.

7 Appendix

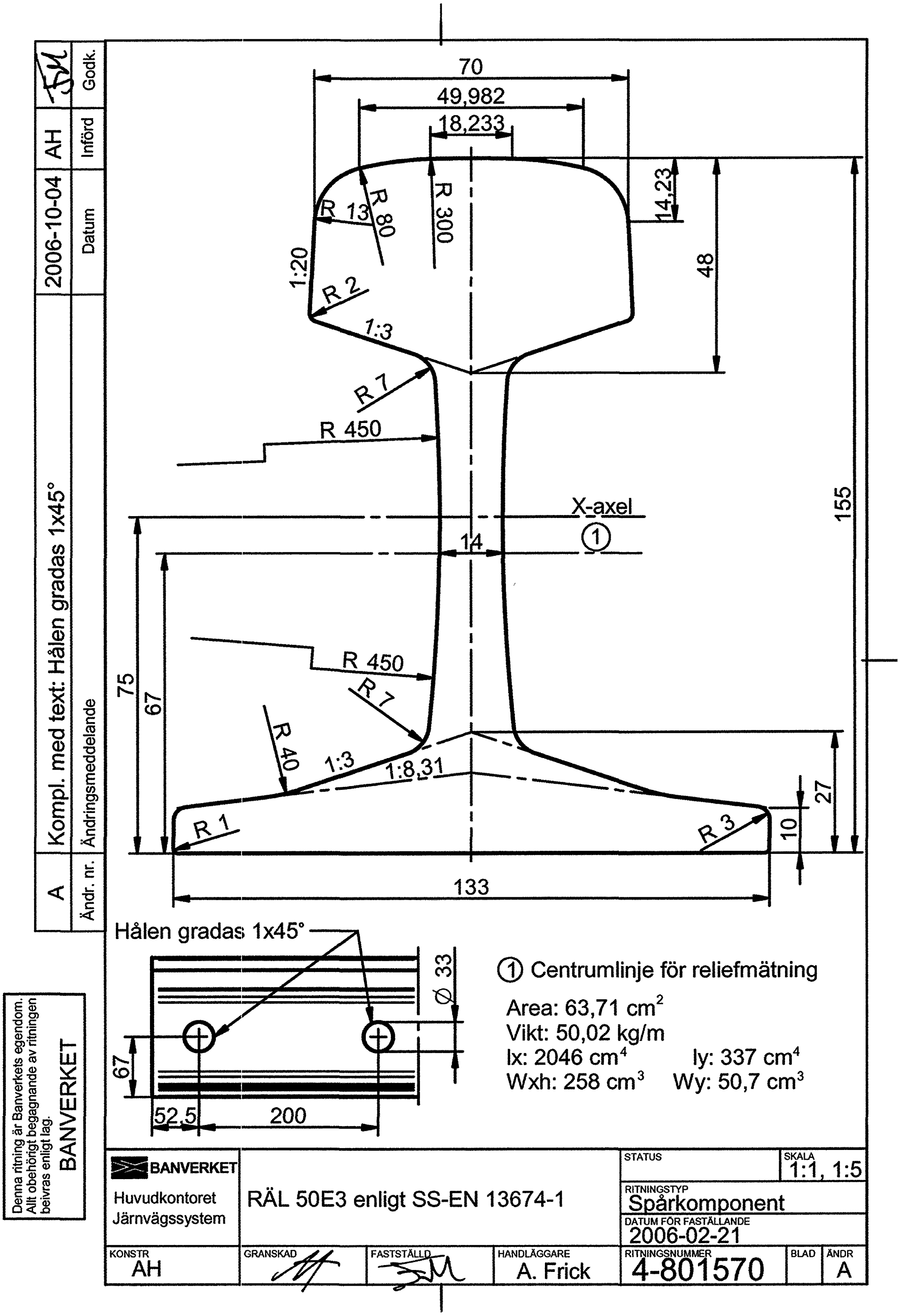

Figure 7.1: Swedish railway administration's drawing of rail profile BV50 / 50E3.

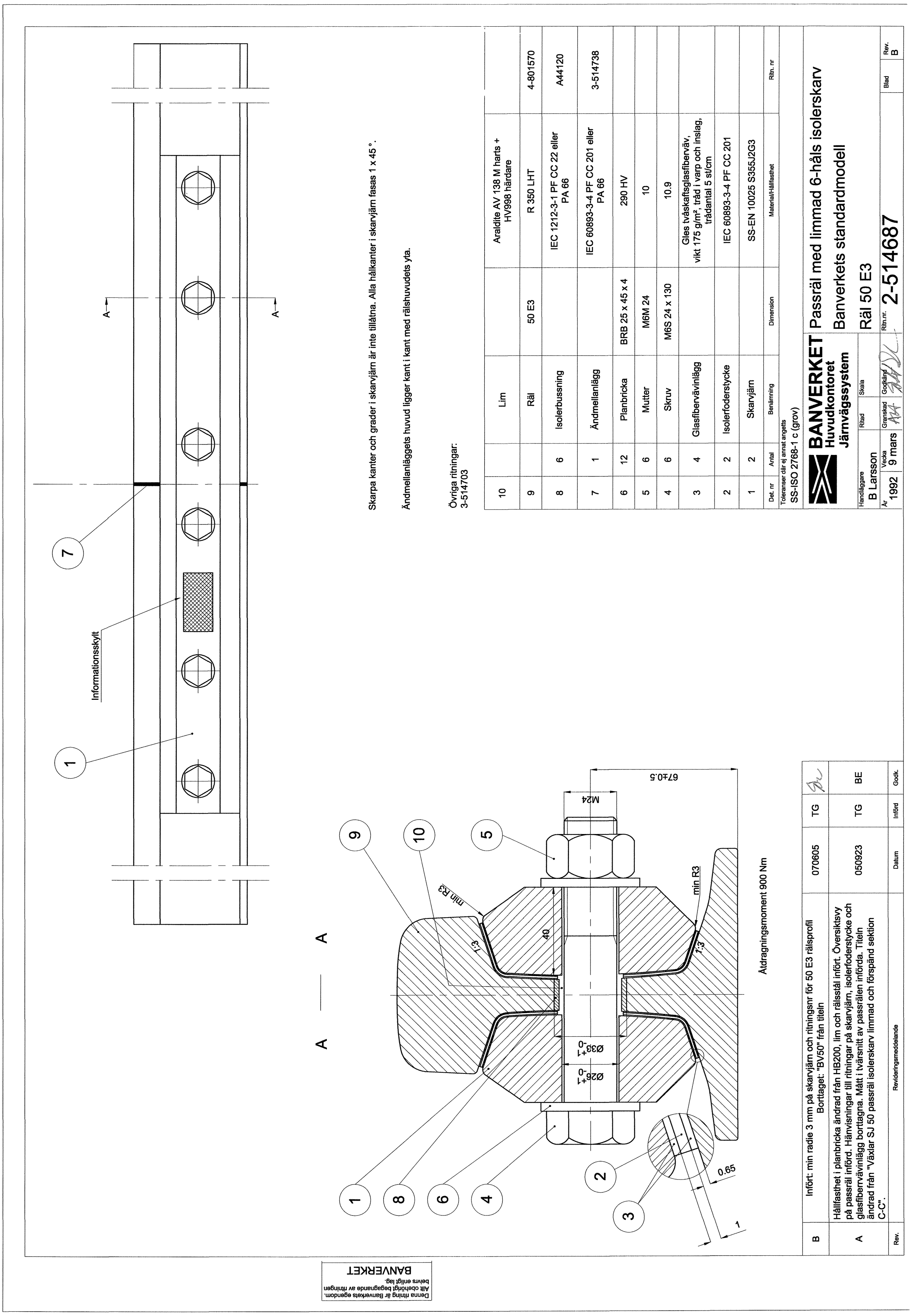

Figure 7.2: Swedish railway administration's drawing of rail including fishplates for profile BV50 / 50E3.

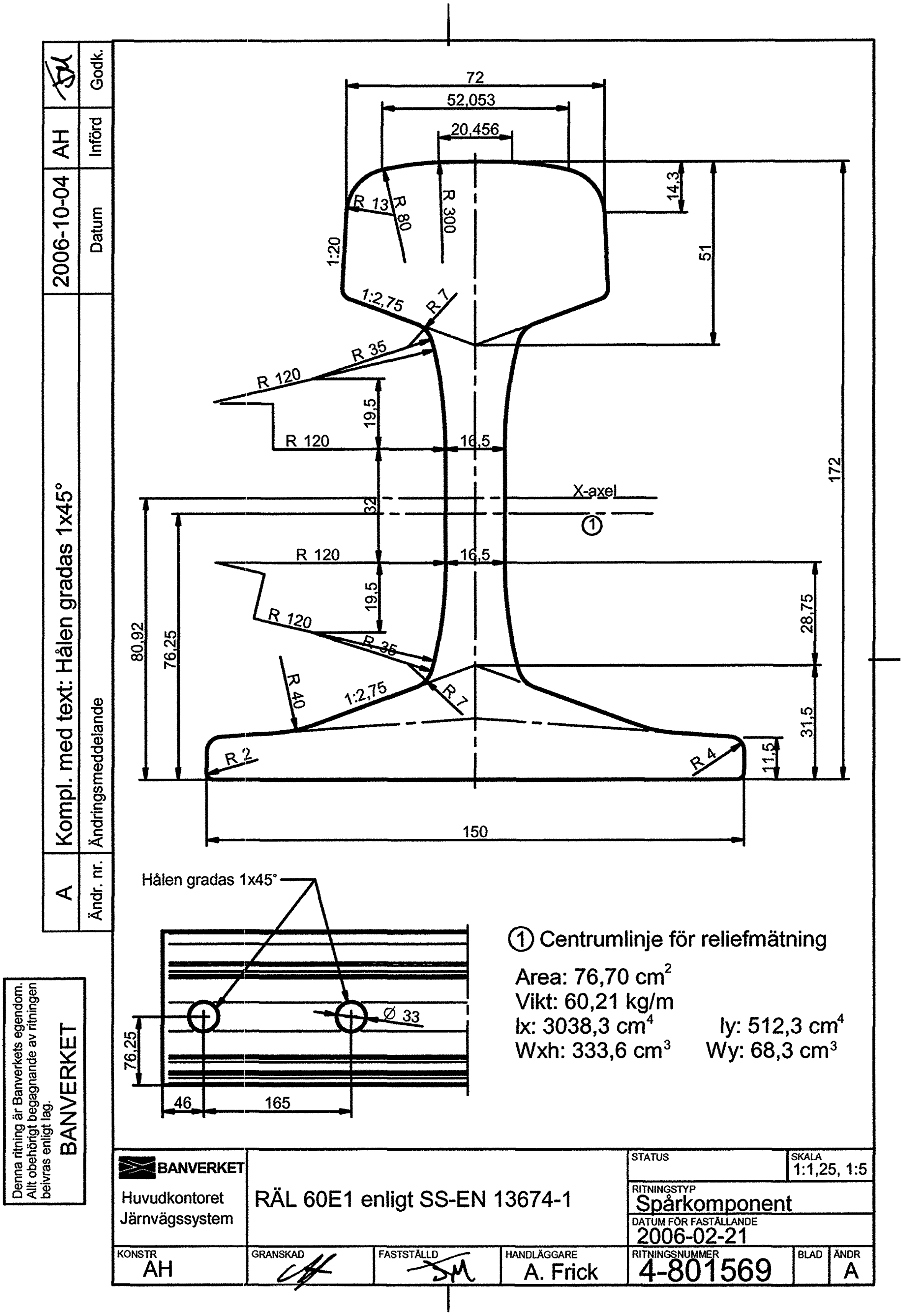

Figure 7.3: Swedish railway administration's drawing of rail profile UIC60 / 60E1.

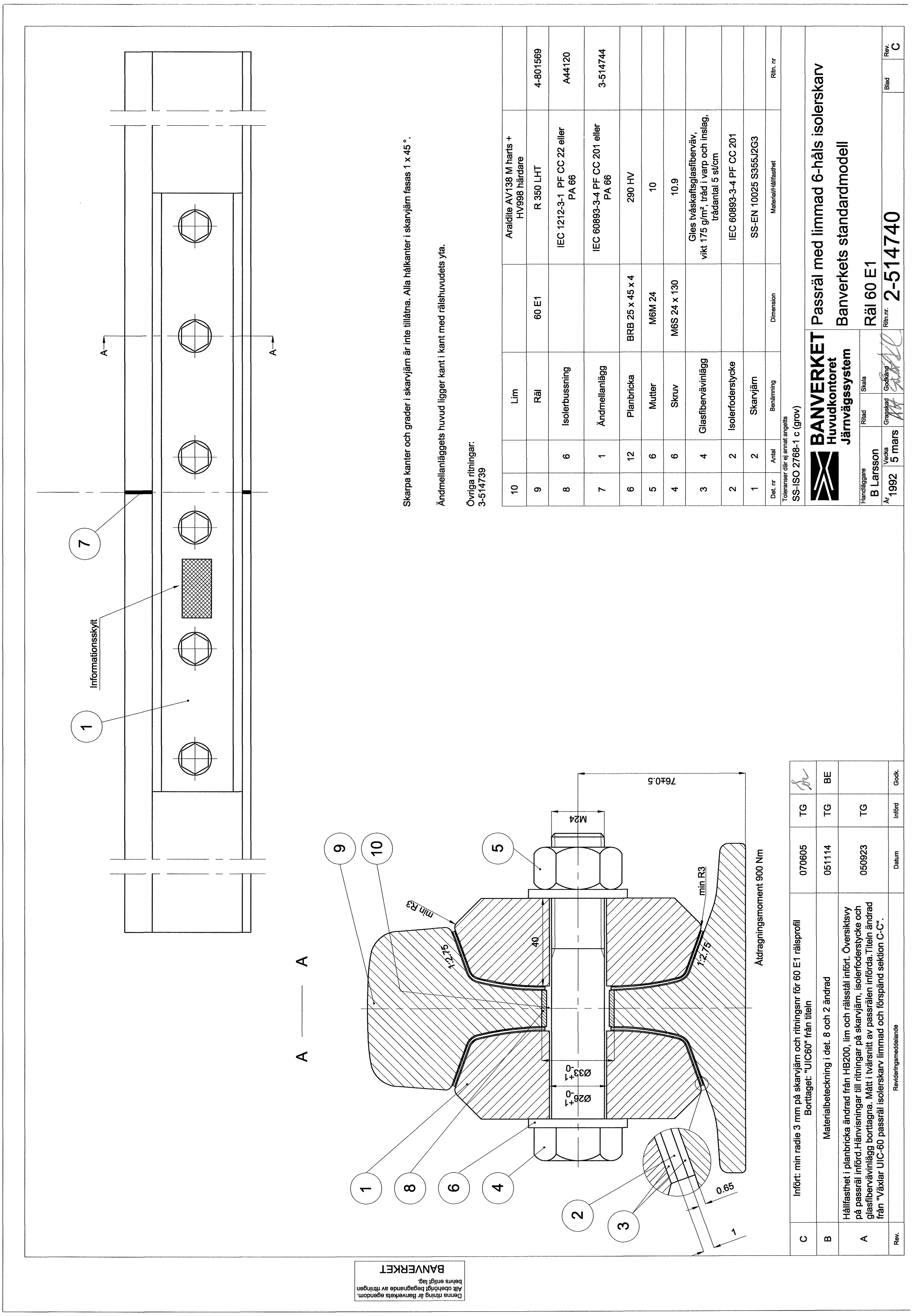

Figure 7.4: Swedish railway administration's drawing of rail including fishplates for profile UIC60 / 60E1.

References

[1] Gunnar Blom and Björn Holmquist. *Statistikteori med tillämpningar*. Studentlitteratur, 1998.

[2] Tore Dahlberg and Anders Ekberg. *Failure Fracture Fatigue An Introduction*. Studentlitteratur, 2002.

[3] Lennart Råde and Bertil Westergren. *Mathematics Handbook for Science and Engineering*. Studentlitteratur, 2004.

[4] Norman E. Dowling. *Mechanical behavior of materials*. Pearson Education, Inc, 2007.

[5] Jens C O Nielsen Elena Kabo and Anders Ekberg. Alarm limits for wheel-rail impact loads – part 1: rail bending moments generated by wheel flats. *Vehicle system dynamics*, 44:718–729, 2006.

[6] Urban Hjorth. *Statistisk slutledning i ekonomi och praktik*. Studentlitteratur, 1998.

[7] Fredrik Jansson. Trv 2010/87382 teknisk kravspecifikation för passräler med limmade isolerskarvar, 2010.

[8] Igor Rychlik and Jesper Rydén. *Probability and Risk Analysis An Introduction for Engineers*. Springer, 2006.

[9] Dassault systems. Abaqus version 6.8. http://www.simulia.com, 2008.